Int J Clin Exp Pathol 2016;9(6):5871-5881
www.ijcep.com /ISSN:1936-2625/IJCEP0021236

Original Article

Impacts of dynamic mechanical stretch on the expression of plasminogen activator inhibitor-1 (PAI-1) in human A549 cells

Yongqing Guo[1], Weiwei Zhang[1], Lina Zheng[1], Weixing Guo[2], Huaping Zhang[3], Xiaona Li[4]

[1]Department of Anesthesiology, Shanxi Provincial People's Hospital, Taiyuan, China; [2]Department of Anesthesiology, Taiyuan Women and Child Health Hospital, Taiyuan, China; [3]Center Laboratory, Shanxi Medical University, Taiyuan, China; [4]Institute of Biomechanics, Taiyuan University of Science and Technology, Taiyuan, China

Received December 5, 2015; Accepted February 15, 2016; Epub June 1, 2016; Published June 15, 2016

Abstract: We investigated the expression of plasminogen activator inhibitor-1 (PAI-1) in A549 cells under cyclic mechanical stretch using cytomechanics. A cell stretch loading device was used to simulate mechanical ventilation conditions towards the *in vitro* cultured A549 cells, with stress loads of 10% and 20% and frequency of 0.3 Hz for 4, 12, and 24 h. Polymerase chain reaction and western blotting were then performed to measure the expression of PAI-1mRNA and protein; annexin V/propidium iodide flow cytometry was performed to detect apoptosis; an enzyme linked immunosorbent assay was performed to detect the expression of interleukin-8 in the supernatant; and electron microscopy was performed to observe changes in cell morphology. The expression of PAI-1mRNA and protein, cell early apoptosis rate, and interleukin-8 expression in the supernatant in each 20% stretch subgroup were increased compared to the corresponding control group, and cell damage was more obvious by electron microscopy observation. Mechanical stretch may damage A549 cells and upregulate PAI-1 expression.

Keywords: Alveolar type II epithelial cells, PAI-1, mechanical stretch, apoptosis

Introduction

During the treatment of acute lung injury and acute respiratory distress syndrome caused respiratory function failure, mechanical ventilation (MV) is an indispensable method; MV is also often applied during general anesthesia in surgeries. However, MV may exacerbate existing lung damage or induce damage in healthy lungs [1, 2]; additionally, short-term MV for only a few hours of general anesthesia may lead to significant changes in pulmonary mechanics and molecular products [3], referred to as ventilator-induced lung injury (VILI). In general, VILI can cause mechanical injury during the early stage, followed by inflammatory cell infiltration and cytokine-mediated biological reaction. Mechanical injury can cause biological damage, which may aggravate the former [4, 5]. Biological injury has now become a research focus, but its pathogenic mechanisms are very complex and require further analysis.

Studies of VILI typically involve animals or *in vitro* lung models. Given the complexity of lung morphology and mechanical properties, it is difficult to explain the sources of inflammatory mediators on an organ level, limiting in-depth analyses. The *in vitro* cell stretch model can eliminate the interference of non-research factors; additionally, the development of cell mechanics can reveal the mechanism of VILI on the cell level [6]. Therefore, we used a Flexercell-4000™ cell stretch loading device to simulate *in vivo* MV caused stretch stress on lung epithelial cells.

A large number of inflammatory cells (such as lung macrophages, neutrophils, and lymphocytes) have been used to study VILI-induced inflammatory responses [7, 8]. However, mammalian alveolar epithelial cells are mainly composed of type II alveolar epithelial cells (ATII) and type I alveolar epithelial cells. ATII cells are responsible for producing surface-active sub-

stances and play an important role in pulmonary host defense; type I epithelial cells are less prevalent and cover most of the gas-exchanging surface of the lung [9]. Foster found that in embryonic lung tissues, static stretch promoted the transformation of ATII cells to type I epithelial cells [10]. The transdifferentiation of ATII cells into type I alveolar epithelial cells is not only related to lung development, but also plays an important role in repairing lung injury [11]. As described above, ATII cells play important roles in lung development and the occurrence and development of diseases; however, freshly isolated ATII cells may have partial or low-level non-associated cell contamination, and the culture process may not maintain their phenotypes, making it difficult to interpret the pathways of MV-induced lung epithelial cell injury [12]. Therefore, we used A549 cells (human-ATII cells strain) because these cells have many characteristics consistent with ATII cells. Morphologically, both cell types grow in a subconfluent state, can hold the cubic form, and synthesize lecithin and phosphatidylcholine [13].

Plasminogen activator inhibitor-1 (PAI-1) is the main inhibitor of urokinase-type plasminogen activator (uPA); PAI-1, uPA, and its receptor uPA receptor (uPAR) constitute the peri-cell fibrinolytic system. These three factors interact with each other and are influenced by the expression of other cytokines to precisely regulate the dynamic equilibrium of extracellular matrix deposition and degradation [14]. Recent studies have shown that in addition to its traditional function of regulating cell fibrinolysis, PAI-1 also regulates cell adhesion, movement, differentiation, and proliferation, thus playing important roles in body immunization and controlling inflammation and infections [15]. Some studies focusing on the roles of PAI-1 in lung inflammation have suggested that PAI-1 might affect lung inflammation. Xiao et al. found that the expression of uPA system components from the sputum culture of patients with chronic obstructive pulmonary disease (COPD) was abnormal, and uPAR and PAI-1 showed significantly higher expression compared to the healthy control group. PAI-1 was significantly negatively correlated with the percentage of the patient's first-second forced expiratory volume to the predicted volume [16]. Wolthuis et al. confirmed that the tidal volume of MV in rats caused the upregulation of PAI-1 in lung tissues, while PAI-1 gene knockout rats showed significantly reduced leukocytic infiltration inside the alveoli compared to normal rats after MV. These results indicate that the role of PAI-1 in VILI induces neutrophils to migrate into the alveoli [17]. However, the impacts of purely mechanical stretching of alveolar epithelial cells on PAI-1 remain unclear.

Interleukin (IL)-8 is an important product of activated epithelial cells and the most important neutrophil chemotactic factor; stimulation by smoking, infection, and other factors, airway epithelium, neutrophils, macrophages, and lymphocytes releases large amounts of IL-8 [14]. Previous studies confirmed that exposure of A549 cells to a 30% stretch amplitude increases IL-8 gene transcription, while exposure below 20% does not increase expression [18]. However, the relationships between IL-8 expression and PAI-1 after mechanical stretching remain unclear.

In this study, we examined the pathogenesis of VILI and verified the roles of PAI-1 in its developmental process. We hypothesized that under highly controlled cyclic mechanical stretching; A549 cells may significantly upregulate the expression of PAI-1 and IL-8 at different stretch strengths and different frequencies over time, which may be accompanied by changes in cell morphology. The purpose of this study was to determine the roles of PAI-1 during the occurrence and development of VILI inflammation to identify new targets for the clinical treatment of VILI.

Materials and methods

Cell culture

The human lung epithelial cell line A549 was purchased from the Shanghai Institute of Cell Bank and cultured and subjected to stretch loading in RPMI1640 containing 10% fetal bovine serum, 100 U/mL penicillin, and 100 μg/mL streptomycin (Gibco, Grand Island, NY, USA) at 37°C and 5% CO_2. The specific procedures were as follows. To logarithmic phase A549 cells, we added 0.25% trypsin solution (Gibco) to cover the cell layer; when the cells began to shrink, became round, or the cell gap was widened, the digestive solution was removed. We added an appropriate amount of

fetal calf serum to terminate the digestion, and then added the appropriate amount of culture medium and gently resuspended the cell by pipetting. The cells were seeded at a density as 5×10^5 cells/mL into collagen basal membrane (collagen I)-coated BioFlex 6-well culture plates (BioFlex, USA) for 24 h culture.

Mechanical stretch and grouping

Before the cyclic stretch test, the culture medium was removed and replaced with fresh 2% serum-containing medium (3 mL/per well). The plates were placed into a Flexercell-4000™ cell loading device (Flexcell International Inc., Hillsborough, NC, USA, automatically controlled using FX-4000 computer software), and then the entire loading device was placed into the incubation box. The non-stretch group was also seeded into 6-well plates and placed in the same incubator as the stretch group. The stretch parameters were expressed as the frequencies and amplitudes, and the amplitudes were determined by the increase in scaled silicone membrane surface area, while the stretch degree of the membrane was determined using the device with an applied vacuum and continuously monitored during experiment. The parameters used in this study were those described previously [6, 19], in which 30% stretching of the lung epithelial cells was equal to 100% of the lung volume (total amount of tidal volume and residual volume); therefore, 10% stretch was set as group I (physiological tidal volume stretch) and 20% stretch as group II (greater than the tidal volume while less than the pulmonary hyperextension [30% stretch]). Considering the impacts of the frequencies on the cells, we selected 0.3 Hz, which was larger than 0.2 Hz (normal respiratory frequency) and less than 0.4 Hz (high-frequency respiration), to simulate high-frequency high-tidal volume ventilation during the MV treatment process and to investigate the influence of long-term high-frequency high-tidal volume ventilation on lung epithelial cells. Therefore, the stretch load parameters in this study were as follows: amplitude: 10% and 20%; frequency: 0.3 Hz; waveform: sine wave. Three subgroups were also evaluated according to the loading time, including 4 h (groups I4s and II4s), 12 h (groups I12s and II12s), and 24 h (groups I24s and II24s); the corresponding non-stretch subgroups were incubated for the same period and included groups I4c and II4c, I12c and II12c, and I24c and II24c.

Annexin V/propidium iodide (PI) flow cytometry

A total of 10^5 cells were harvested by trypsinization, rinsed twice with PBS, and then rinsed once with binding buffer; the cells were then resuspended in 200 μL of binding buffer, combined with 5 μL of annexin V-FITC reagent (Yeasen, Shanghai, China), and incubated in the dark at room temperature for 15-20 min; 10 μL of PI (50 μg/mL) and 200 μL of binding buffer were added followed by flow cytometric analysis (FACS Calibur, BD Biosciences, Franklin Lakes, NJ, USA).

Detection of PAI-1mRNA expression by RT-PCR

The cells were collected, combined with 1 mL of Trizol (Invitrogen, Carlsbad, CA, USA), and repeatedly mixed with a 1-mL syringe to fully lyse and dissolve the cells to extract the RNA. We then added 200 μL of chloroform, agitated the mixture vigorously for 30 s, and centrifuged the sample at 4°C and 12,000 rpm for 5 min. We then transferred the supernatant to another EP tube, added an equal volume of isopropanol, and incubated the sample at room temperature for 5 min. The mixture was centrifuged at 4°C and 12,000 rpm for 5 min to precipitate the RNA. The precipitate was rinsed with 1 mL of 70% ethanol twice and then centrifuged at 4°C and 12,000 rpm for 2 min. RNA that had precipitated at the bottom of the tube was dissolved in 50 μL of 0.1% DEPC water for use as the template for reverse transcription.

First, 11 μL of RNA (1 μg) and 1 μL of random primers (0.2 μg/mL) were incubated at 65°C for 5 min. Next, we added 4 μL 5 × buffer, 3 μL of dNTP (10 mM), 1 μL of RNA inhibitor (20 U/μL), and 1 μL of reverse transcriptase (20 U/μL) (Fermentas, Vilnius, Lithuania) and incubated the sample at 25°C for 10 min, 42°C for 1 h, and 72°C for 15 min.

The β-actin and PAI-1 primers designed by our lab and synthesized by Shanghai Bio Tech, Ltd. (Shanghai, China). The primer sequences were as follows: β-actin: upstream primer: 5'-agagctacgagctgcctgac-3'; downstream primer: 5'-agcactgtgttggcgtacag-3'; product fragment: 184 bp. PAI-1 upstream primer: 5'-ctctctctgccctcaccaac-3'; downstream primer: 5'-gtggagag-

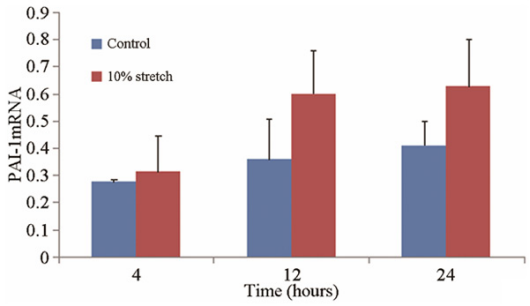

Figure 1. PCR results of the expressions of PAI-1mRNA in group I, the control group, group I4s, I12s, and I24s, respectively. Compared with the control group, the expressions of PAI-1mRNA in the other three groups showed no significant difference.

gctcttggtctg-3', product fragment: 212 bp. Ten microliters of FastStart Universal SYBR Green Master (ROX; Roche, Basel, Switzerland) was mixed with 0.5 μL of upstream primer (15 μM), 0.5 μL of downstream primer (15 μM), 2 μL of cDNA, and 7 μL of non-DNAse and RNAse water in a total volume of 20 μL. The PCR conditions were as follows: denaturation at 94°C for 10 min to activate the Tag enzyme, followed by 94°C for 15 s, 60°C for 60 s, for a total of 45 cycles. Fluorescence quantitative PCR (Roche) was performed to read the CT value (cycle threshold). First, the difference between CT values of the target X gene in each sample and the internal β-actin gene were calculated as ΔCT = CT(X)-CT (β-actin); second, we used the ΔCT value of each sample in the experimental groups to subtract the ΔCT value of the control group, generating ΔΔCT; third, we used $2^{-\Delta\Delta CT}$ to calculate [19] the fold-change of expression of the X gene in the experiment group compared to that in the control group.

Expression detection of PAI-1 protein by western blotting

The culture medium was removed and the cells were rinsed with PBS once; we added PIPA (Beijing BioTeke Co., Ltd., China) to fully lyse the cells on ice and then added PMSF at a final concentration of 1 mM to the protein sample. The sample was centrifuged at 10,000 × *g* and 4°C for 5 min to separate the supernatant, which was stored at -80°C (preparation of 100 mM PMSF: weighed 0.176 g of PMSF and dissolved in 1 mL of isopropanol, full pipetted, and prepared immediately before use). Proteins were analyzed by SDS-PAGE under the following conditions: concentration gel was run at 80 V constant voltage for approximately 45 min; the separation gel was run at a constant voltage of 120 V for approximately 3 h. The proteins were then electrically transferred onto a nitrocellulose membrane (PVDF) at 100 mA for 1 h, blocked overnight in 5% BSA solution at 4°C, and incubated with the primary antibodies overnight at 4°C, including mouse-derived β-actin (C4): sc-47778, rabbit-derived PAI-1 (H-1135): sc-8979 (Beijing Biosynthesis Biotechnology Co., Ltd.), which were both diluted to 1:1000 with Tris-buffered saline containing Tween 20. The blots were incubated with secondary antibodies at room temperature for 2 h: anti-mouse secondary antibody or anti-rabbit secondary antibody, both diluted 1:10,000. Blots were developed by electrochemiluminescence, scanned, and analyzed (GelDoc XR Gel Documentation System, Analysis Software: Quantity One, Bio-Rad, Hercules, CA, USA).

Expression detection of IL-8 by enzyme linked immunosorbent assay (ELISA)

The supernatant of the cells was collected to detect the OD value of IL-8 according to the instructions of the human IL-8ELISA kit (Beijing 4A Biotech Co., Ltd.); the OD value at 492 nm was then set as the abscissa, with the concentration of the standard as the ordinate, to prepare a standard curve on a double logarithmic scale; the concentration of the sample was then determined from the standard curve according to its OD value.

Structure observation of the A549 cells by electron microscopy

The cell suspension was centrifuged at 1000 rpm for 5 min; the precipitate was then fixed with 2.5% glutaraldehyde, rinsed with PBS, dehydrated with acetone, post-fixed with 1% osmium tetroxide, embedded with epoxy resin, and stained with aluminum citrate; the samples were then observed by electron microscopy for analysis (provided by the electron microscopy room of Shanxi Medical University).

Statistical analysis

Independent experiments were repeated three times. The expressions of genes and proteins in each group were the ratio of the related value to that of β-actin; therefore, the results indicate

Table 1. The PAI-mRNA expressions in the A549 cells of group I (n = 3, $\bar{x}$ ± s)

Group	4 h	12 h	24 h
Control group	0.275 ± 0.008	0.358 ± 0.151	0.410 ± 0.087
Stretch group	0.312 ± 0.135	0.600 ± 0.159	0.626 ± 0.176

Note: Compared with the control group, the expressions of PAI-1mRNA among the stretch subgroups showed no significant difference.

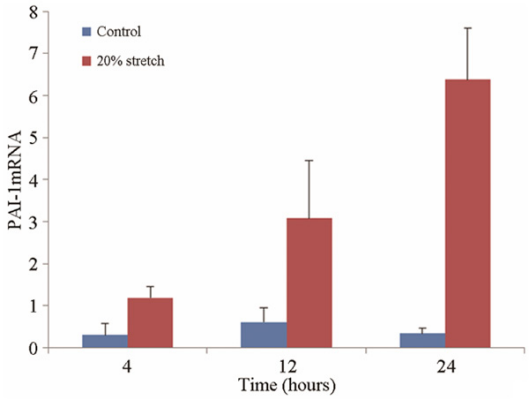

Figure 2. PCR results of the expressions of PAI-1mRNA in group II, the control group, group II4s, II12s, and II24s, respectively. Compared with the control group, the expressions of PAI-1mRNA in the other three groups were significantly increased, while only group II24s showed significant difference. Compared with the corresponding control group ($^aP < 0.01$).

relative expression levels. SPSS 15.0 software was used for data analysis (SPSS, Inc., Chicago, IL, USA) and measurement data were expressed as the mean ± standard deviation ($\bar{x}$ ± s). Intergroup comparison was performed ANOVA (Scheffe test) and the pairwise comparison with the SNK test, with a = 0.05 and $P < 0.05$ considered as statistically significant differences.

Results

Expression of PAI-1mRNA

The expression of PAI-1mRNA in group I at different time points showed no significant differences with the corresponding control group (**Figure 1**; **Table 1**), while expression in group II only exhibited significant differences between group II24s and II24c ($P < 0.01$) (**Figure 2**; **Table 2**). No statistically significant difference was observed between the values at 4 h and 12 h, and the expression of PAI-1mRNA were increased compared to in the control group (0.302 ± 0.283, 0.609 ± 0.339) by 4-fold (1.192 ± 0.255) and 5-fold (3.078 ± 1.380), respectively (**Figures 1**, **2**; **Tables 1**, **2**).

Expression of PAI-1 protein in group II

Western blotting analysis showed no statistically significant difference in the expression of PAI-1 protein between group II and the corresponding control group, which may because protein expression was regulated by genes, resulting in a lag effect; as stretch time increased, expression increased, and the difference in PAI-1 protein expression between group II24s and II24c was less than 1-fold (0.928 ± 0.073, 0.507 ± 0.124) (**Figure 3**; **Table 2**).

Cell apoptosis in group II

The early apoptosis rates in the three stretch groups were increased compared to in the corresponding control groups; although the differences were not statistically significant, the values exhibited an increasing trend. For example, the value in group II24s was increased by nearly two-fold compared to that in group II24c (**Figure 4**; **Table 2**).

Results of IL-8 detection in group II by ELISA

After the A549 cells were stimulated by 20% mechanical stretch, compared with the corresponding control groups, the expression of IL-8 in groups II4s, II12s, and II24s was significantly increased ($P < 0.01$); the expression exhibited a time-dependent increasing trend, which was particularly obvious at 24 h (11.575 ± 1.010 and 159.464 ± 19.715) (**Figure 5**; **Table 2**).

Results of electron microscopy in group II

The cell morphology in group II4c was similar to that in normal cells: the cells were more regular, cubic or round, and contained large numbers of microvilli in varying lengths on the surface; the nuclei were obvious and round; the cytoplasm was lightly stained, containing many mitochondria, with a rough endoplasmic reticulum, Golgi complex, and lysosomes. The cell morphologies of groups II12c and II24c changed very little, showing slight edematous organelles. The morphological changes in groups I and II were significant, among which the

Table 2. Expressions of PAI-1mRNA, PAI-1 protein, and IL-8 in the A549 cells of group II ($\bar{x} \pm s$)

Group	PAI-1mRNA	PAI-1 protein	IL-8 (pg/ml)	Early apoptosis rate (%)
II4c	0.302 ± 0.283	0.533 ± 0.153	7.203 ± 0.904	1.660 ± 1.339
II4s	1.192 ± 0.255	0.516 ± 0.153	32.167 ± 3.580[a]	3.337 ± 0.275
II12c	0.609 ± 0.339	0.527 ± 0.173	9.023 ± 1.488	0.657 ± 0.131
II12s	3.078 ± 1.380	0.796 ± 0.147	91.965 ± 11.787[a]	1.053 ± 0.061
II24c	0.338 ± 0.127	0.507 ± 0.124	11.067 ± 1.333	2.873 ± 1.125
II24s	6.378 ± 1.222[a]	0.928 ± 0.073	146.473 ± 6.934[a]	5.910 ± 2.582
N	3	3	3	3

Note: Compared with the corresponding control group, [a]$P < 0.05$.

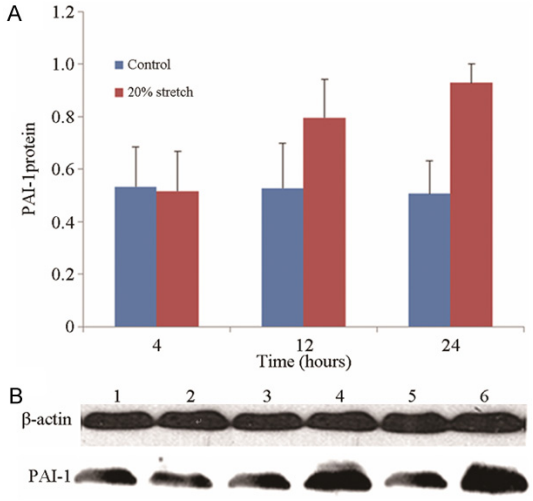

Figure 3. Western-blot results of the PAI-1 protein expressions in the cells, compared with the corresponding control group, the expressions of the PAI-1 protein in the three groups showed no significant difference ($P > 0.05$).

changes in group II24s were the most prominent: the cells swelled, the microvilli on cell surface were reduced, the nuclei shrank, the mitochondria swelled, and the cristae ruptured, disappeared, disintegrated, and occurred vacuolization. The rough endoplasmic reticulum expanded and the polyribosomes depolymerized (**Figure 6**).

Discussion

The normal pulmonary respiratory rate at rest is approximately 20 beats/min; the stretch by 8-12% mechanical tensile strength should increase the surface area of the lung epithelial cells by 25%, equivalent to those under physiologic MV, while a stretch of 17-22% mechanical tensile strength should increase the cell surface area by 37-50%, equivalent to those in MV with pathological tidal volume. This can lead to cell apoptosis and death [20]. Ether and Liu confirmed that the MV with low tidal volume (6 and 7.5 mL/kg) does not cause lung damage, while MV with a large tidal volume (15 and 30 mL/kg) causes a series of inflammatory changes in the lung [17, 21]. In this study, we used stretch modes, including high and low stretch, in which 10% mechanical stretch would not alter PAI-1 expression. This is consistent with the fact that low tidal volume does not cause lung damage. Shu also confirmed that when the A549 cells were mechanically stretched, 20% stretch caused apoptosis, while 6% stretch did not affect cell viability [6]. MV with an amplitude of 20% and frequency of 0.3 Hz belonged to the level of high-tidal volume and high-frequency, which is easy to achieve when performing MV towards the damaged lungs. Additionally, the MV supporting patients with lung injury is often used long-term, so we to evaluated the results of mechanical stretch stimulation towards the A549 cells at 4, 12, and 24 h, which was consistent with clinicopathological processes.

The forms of cell stretch are typically expressed as the stretch amplitude and frequency, and the entire process can be accurately calculated using the Flexercell-4000™ system software. The amplitude was expressed as the increase in the surface area of the standardized collagen basal membrane, and stretch ranges were determined by the standardized vacuum applied on the surface of the basal membrane, which was closely monitored throughout the process. Hammerschmidt et al used this system to stretch ATII cells to evaluate the impacts of different stretch amplitudes and frequencies on cell viability, including cyclooxygenase-2, 5-lipoxygenase, and nitric oxide synthase of endothelial cells [20]. Shu used this system to stretch A549 cells to evaluate the impacts of different stretch amplitudes and stretching times on the expression of pentraxin-3 [6]. Advanced equipment and collagen basal mem-

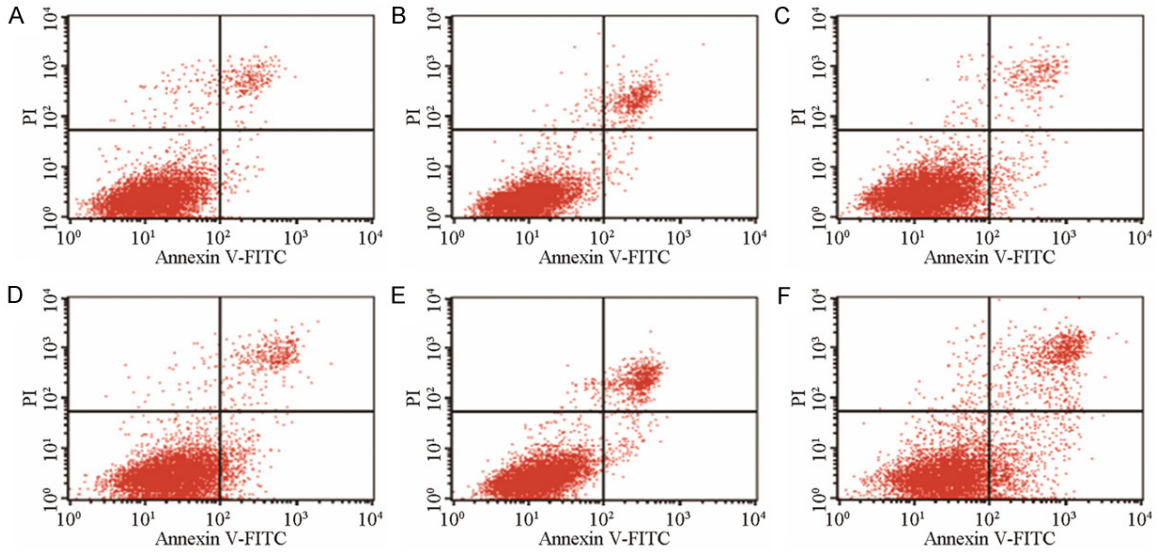

Figure 4. Representative results of Annexin V/PI staining flow cytometry after stretch. The abscissa was Annexin V FITC, and the ordinate was PI. The negative results for both Annexin V and PI occurred in the alive cells (lower left quadrant), the early apoptotic cells exhibited negative PI accompanied with Annexin V (lower right quadrant); the late apoptotic cells exhibited positive PI accompanied with Annexin V (upper right quadrant); and the dead cells exhibited positive PI while not accompanied with Annexin V (upper left quadrant). (A-C) were the results of the control group at 4 h, 12 h, and 24 h, while (D-F) were the results of the stretch group at the three time points.

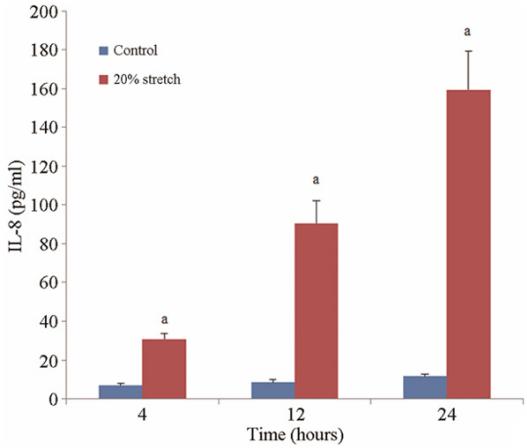

Figure 5. The concentrations of IL-8 in the supernatant of group II, the control group, group II4s, II12s, and II24s, respectively. Compared with the corresponding control group, the IL-8 expressions in the three groups were significantly increased ($^{a}P < 0.01$).

brane-coated plates were used to determine the precise controllability of the entire stretch process, ensuring the success of this experimental modeling process.

The results of this experiment confirmed that high-amplitude and high-frequency mechanical stretch leads to increased PAI-1mRNA expression in A549 cells, and with increasing stretch amplitude and time, the expression level gradually increased. Mechanical stretch of 20% for 4 h significantly increased PAI-1 gene expression, suggesting that PAI-1 is a relatively early sensitive gene during VILI. Additionally, the expression of PAI-1 protein was correspondingly increased, but no significant difference was found among different stretch groups (though the values exhibited an increasing trend), which may because protein generation is the result of gene regulation, resulting in a delay. Lipopolysaccharide and cigarette smoke extract were used to stimulate A549 cells for 24 h, which caused the expression of PAI-1mRNA in the alveolar epithelium to significantly increase. Western blotting only showed the increased expression of PAI-1 protein 48 h later, supporting the results of this study [14].

Because PAI-1 is the main inhibitor of PA and plays an important role in the formation of fibrin, previous studies have focused on its profibrotic effects. However, in recent years, the pro-inflammatory effects of PAI-1 have also gained attention, and studies suggest that the fibrinolytic system affects lung inflammations. Rats with uPAR deficiency produce different inflammatory cells and show the migration of

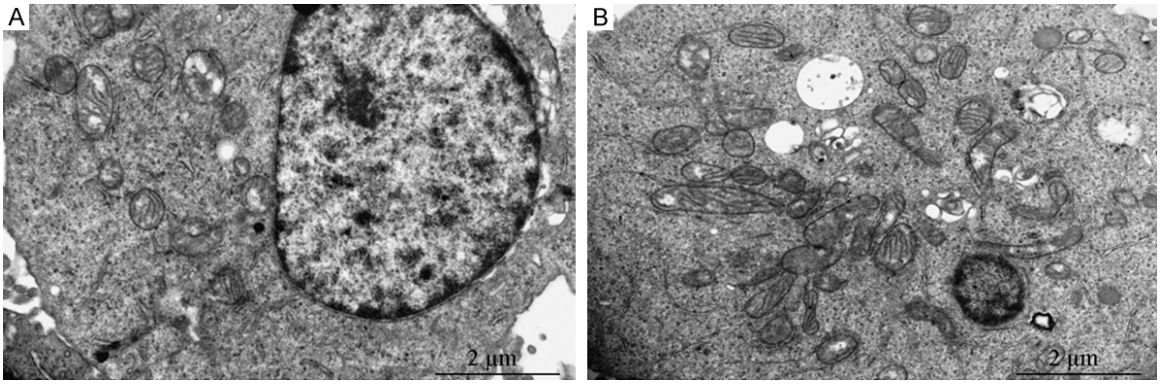

Figure 6. Electron microscopic results of group II24s. A: Image of group II24s: the cells swelled, the microvilli on cell surface were reduced; the nuclei shrank; the mitochondria swelled, and the cristae ruptured, disappeared, disintegrated and underwent vacuolization; the rough endoplasmic reticulum expended and the polyribosomes depolymerized. B: Image of the control group of group II24s: the cells showed basically normal morphologies, the nuclear membrane was intact, and the mitochondrial cristae were obvious.

a large number of damaged leukocytes [22]. PAI-1 may also affect the transportation of the neutrophils in many ways; in fact, PAI-1 is not only a uPA inhibitor in the lungs, but also interferes with cell adhesion in a more direct way, thus promoting neutrophil aggregation [23]. In addition, the biological studies of tumor cells supported the roles of PAI-1 in the process of cell proliferation. The high expression of PAI-1 indicated that the tumor had high invasion and metastasis abilities, and thus was an indicator of poor prognosis [24, 25]. Rats with a silenced PAI-1 gene exhibited less neutrophil accumulation in the lungs after MV, and PAI-1 was more sensitive for detecting VILI than were other biomarkers [17]. Different studies have shown that PAI-1 is upregulated in a variety of inflammation processes. In a mouse model of *Klebsiella pneumoniae*, infection with the bacilli for 24 h increased PAI-1 in the lung tissues by 9-fold, and 7-fold 48 h later [26]. In the induced sputum of COPD patients, PAI-1 was also nearly 10-fold higher than in the normal control group [16]. Our study also found that after 24 h of 20% stretch, the expression of PAI-1mRNA was increased by 20-fold compared to the control group.

The expression of PAI-1 may be regulated by a number of inflammatory cytokines (such as IL-1, IL-6, tumor necrosis factor-α), transforming growth factor-β, and epidermal growth factor [21, 27]. PAI-1, in turn, may also affect the levels of a variety of inflammatory factors. IL-8 is a chemokine that allows neutrophils to penetrate the endothelial cells and aggregate, but IL-8 secreted by endothelial cells of the normal human umbilical vein bind heparin sulfate and syndecan-1 to form the molecule complex, which may decrease neutrophilic chemotaxis. PAI-1 can stabilize the chemotaxis form of IL-8, thus inhibiting the generation of the molecular complex and increasing neutrophilic accumulation. Therefore, PAI-1 can be used as a target for treating inflammation [28]. IL-8 is an inflammatory cytokine with significant chemotactic effects during the inflammatory process of COPD. PAI-1 can regulate IL-8 expression; IL-8 can induce inflammatory effects, including inflammatory cell recruitment. This increases the release of PAI-1, which is critical for the formation of the COPD inflammatory factor network and promotes and maintains COPD inflammation [14]. Additionally, PAI-1 itself shows chemotaxis on inflammatory cells, and Renchens et al found that PAI-1 mediates neutrophilic recruitment by promoting the activity of JNK, promoting cell migration [29]. In this study, the increased expression of PAI-1 was also accompanied by increased secretion of IL-8, suggesting that mechanical stretching of A549 cells produced the early inflammatory cytokine PAI-1. The expression of its downstream neutrophil chemokine IL-8 was also activated; IL-8 recruits a large number of inflammatory mediators in endothelial cells, thus increasing cell damage, which was clearly observed by electron microscopy. After 24 h of 20% stretch, the cells swelled significantly and the microvilli on the cell surface were reduced. The nuclei shrank,

the mitochondria swelled, and the cristae ruptured, disappeared, disintegrated, and showed vacuolization. The rough endoplasmic reticulum expended and the polysomes depolymerized; this cellular damage further induced the re-expression of PAI-1, thus forming a network of inflammatory responses, finally resulting in severe acute damage and the structural degeneration of the cells.

In this study, we only examined the results of pure mechanical stretch towards normal (not damaged) A549 cells, and found that 4 h stretch increased PAI-1 gene expression, indicating that PAI-1 is a sensitive indicator of mechanical stretch-induced biological damage in lung epithelial cells. As the stretch time increased, larger amounts of PAI-1 were generated, suggesting that the generation and quantity of PAI-1 is correlated to the degree of cell damage. In clinical courses, increasing PAI in the lungs of patients with pneumonia was closely related with poor prognosis [30, 31]; furthermore, increasing plasma PAI-1 levels in patients with acute lung injury/acute respiratory distress syndrome was related to increased morbidity and mortality [32]. However, the exact mechanisms regarding how simple mechanical stretching of A549 cells produced PAI-1, activated IL-8, caused aggregation of downstream inflammatory factors, and eventually led to morphological changes of lung epithelial cells require further analysis.

In summary, simple cyclic mechanical stretch of A549 cells induced the expression of PAI-1, which also changed with stretch amplitude and time. PAI-1 appeared to be a sensitive early biological indicator for monitoring VILI, and may increase the degree of lung injury by influencing the expression of IL-8, which may make it a new target for the clinical treatment of VILI.

Acknowledgements

Thanks should be given for the technical assistance provided by Professor Weiyi Chen and Professor Xiaona Li, Institute of Applied Mechanics and Biomedical Engineering, Taiyuan, and Professor Huaping Zhang, Center Laboratory of Shanxi Medical University. This work was funded by Research Project Supported by Shanxi Scholarship Council of China (No. 104).

Disclosure of conflict of interest

None.

Address correspondence to: Yongqing Guo, Department of Anesthesiology, Shanxi Provincial People's Hospital, Taiyuan 030012, Shanxi, China. Tel: +86 351 4960427; Fax: +86 351 4960184; E-mail: docyongqingguo@163.com

References

[1] Kuipers MT, Aslami H, Tuinman PR, De Boer A, Jongsma G and Van der Sluijs K. The receptor for advanced glycation end products in ventilator-induced lung injury. Intensive Care Med Exp 2014; 2: 22.

[2] Vaneker M, Halbertsma FJ, van Egmond J, Netea MG, Dijkman HB, Snijdelaar DG, Joosten LA, van der Hoeven JG and Scheffer GJ. Mechanical ventilation in healthy mice induces reversible pulmonary and systemic cytokine elevation with preserved alveolar integrity: an in vivo model using clinical relevant ventilation settings. Anesthesiology 2007; 107: 419-426.

[3] Ochiai R. Mechanical ventilation of acute respiratory distress syndrome. J Intensive Care 2015; 3: 25.

[4] Wu J, Yan Z, Schwartz DE, Yu J, Malik AB and Hu G. Activation of NLRP3 inflammasome in alveolar macrophages contributes to mechanical stretch-induced lung inflammation and injury. J Immunol 2013; 190: 3590-3599.

[5] Emr B, Gatto LA, Roy S, Satalin J, Ghosh A, Snyder K, Andrews P, Habashi N, Marx W, Ge L, Wang G, Dean DA, Vodovotz Y and Nieman G. Airway pressure release ventilation prevents ventilator-induced lung injury in normal lungs. JAMA Surg 2013; 148: 1005-1012.

[6] Wu Q, Shu H, Yao S and Xiang H. Mechanical stretch induces pentraxin 3 release by alveolar epithelial cells in vitro. Med Sci Monit 2009; 15: BR135-140.

[7] Frank JA, Wray CM, McAuley DF, Schwendener R and Matthay MA. Alveolar macrophages contribute to alveolar barrier dysfunction in ventilator-induced lung injury. Am J Physiol Lung Cell Mol Physiol 2006; 291: L1191-1198.

[8] Kass DJ, Yu G, Loh KS, Savir A, Borczuk A, Kahloon R, Juan-Guardela B, Deiuliis G, Tedrow J, Choi J, Richards T, Kaminski N and Greenberg SM. Cytokine-like factor 1 gene expression is enriched in idiopathic pulmonary fibrosis and drives the accumulation of CD4+ T cells in murine lungs: evidence for an antifibrotic role in bleomyoin injury. Am J Pathol 2012; 180: 1963-1978.

[9] Zhao CZ, Fang XC, Wang D, Tang FD and Wang XD. Involvement of type II pneumocytes in the pathogenesis of chronic obstructive pulmonary disease. Respir Med 2010; 104: 1391-1395.
[10] Foster CD, Varghese LS, Gonzales LW, Margulies SS and Guttentag SH. The Rho pathway mediates transition to an alveolar type I cell phenotype during static stretch of alveolar type II cells. Pediatr Res 2010; 67: 585-590.
[11] Chuquimia OD, Petursdottir DH, Periolo N and Fernández C. Alveolar epithelial cells are critical in protection of the respiratory tract by secretion of factors able to modulate the activity of pulmonary macrophages and directly control bacterial growth. Infect Immun 2013; 81: 381-389.
[12] Letsiou E, Sammani S, Zhang W, Zhou T, Quijada H, Moreno-Vinasco L, Dudek SM and Garcia JG. Pathologic mechanical stress and endotoxin exposure increases lung endothelial microparticle shedding. Am J Respir Cell Mol Biol 2015; 52: 193-204.
[13] Ning QM, Sun XN and Zhao XK. Role of mechanical stretching and lipopolysaccharide in early apoptosis and IL-8 of alveolar epithelial type II cells A549. Asian Pac J Trop Med 2012; 5: 638-644.
[14] Xu X, Wang H, Wang Z and Xiao W. Plasminogen activator inhibitor-1 promotes inflammatory process induced by cigarette smoke extraction or lipopolysaccharides in alveolar epithelial cells. Exp Lung Res 2009; 35: 795-805.
[15] Hildenbrand R, Gandhari M, Stroebel P, Marx A, Allgayer H and Arens N. The urokinase-system role of cell proliferation and apoptosis. Histol Histopathol 2008; 23: 227-236.
[16] Xiao W, Hsu YP, Ishizaka A, Kirikae T and Moss RB. Sputum cathelicidin, urokinase plasminogen activation system components, and cytokines discriminate cystic fibrosis, COPD, and Asthema inflammation. Chest 2005; 128: 2316-2326.
[17] Wolthuis EK, Vlaar AP, Hofstra JJ, Roelofs JJ, de Waard V, Juffermans NP and Schultz MJ. Plasminogen activator inhibitor-type 1 gene deficient mice show reduced influx of neutrophils in ventilator-induced lung injury. Crit Care Res Pract 2011; 2011: 217896.
[18] Vlahakis NE, Schroeder MA and Limper AH. Stretch induces cytokine release by alveolar epithelial cells in vitro. Am J Physiol 1999; 277: L167-173.
[19] Pfaffl MW. A new mathematical model for relative quantification in real-time RT-PCR. Nucleic Acids Res 2001; 29: e45.
[20] Hammerschmidt S, Kuhn H, Sack U, Schlenska A, Gessner C, Gillissen A and Wirtz H. Mechanical stretch alters alveolar type II cell mediator release toward a proinflammatory pattern. Am J Respir Cell Mol Biol 2005; 33: 203-210.
[21] Liu YY, Liao SK, Huang CC, Tsai YH, Quinn DA and Li LF. Role for nuclear factor-kappa B in augmented lung injury because of interaction between hyperoxia and high stretch ventilation. Transl Res 2009; 154: 228-240.
[22] Rijneveld AW, Levi M, Florquin S, Speelman P, Carmeliet P and van Der Poll T. Urokinase receptor is necessary for adequate host defense against pneumococcal pneumonia. J Immunol 2002; 168: 3507-3511.
[23] Zhang YP, Wang WL, Liu J, Li WB, Bai LL, Yuan YD and Song SX. Plasminogen activator inhibitor-1 promotes the proliferation and inhibits the apoptosis of pulmonary fibroblasts by Ca^{2+} signaling. Thromb Res 2013; 131: 64-71.
[24] To M, Takagi D, Akashi K, Kano I, Haruki K, Barnes PJ and Ito K. Sputum plasminogen activator inhibitor-1 elevation by oxidative stress-dependent nuclear factor-kB activation in COPD. Chest 2013; 144: 515-521.
[25] Lupu-Meiri M, Geras-Raaka E, Lupu R, Shapira H, Sandbank J, Segal L, Gershengorn MC and Oron Y. Knock-down of plasminogen-activator inhibitor-1 enhances expression of E-cadherin and promotes epithelial differentiation of human pancreatic adenocarcinoma cells. J Cell Physiol 2012; 227: 3621-3628.
[26] Hoshino Y, Mio T, Nagai S, Miki H, Ito I and Izumi T. Cytotoxic effects of cigarette smoke extract on an alveolar type II cell-derived cell line. Am J Physiol Lung Cell Mol Physiol 2001; 281: L509-516.
[27] Wang ZY, Wu SN, Zhu ZZ, Yang BX and Zhu X. Inhaled unfractionated heparin improves abnormalities of alveolar coagulation fibrinolysis and inflammation in endotoxemia-induced lung injury rats. Chin Med J 2013; 126: 318-324.
[28] Marshall LJ, Ramdin LS, Brooks T, DPhil PC and Shute JK. Plasminogen activator inhibitor-1 supports IL-8 mediated neutrophil transendothelial migration by inhibition of the constitutive shedding of endothelial IL-8/Heparan sulfate/syndecan-1 complexes. J Immunol 2003; 171: 2057-2065.
[29] Luo F, Zhuang Y, Sides MD, Sanchez CG, Shan B, White ES and Lasky JA. Arsenic trioxide inhibits transforming growth factor-β1-induced fibroblast to myofibroblast differentiation in vitro and bleomycin induced lung fibrosis in vivo. Respir Res 2014; 15: 51.
[30] Sapru A, Hansen H, Ajayi T, Brown R, Garcia O, Zhuo H, Wiemels J, Matthay MA and Wiener-Kronish J. 4G/5G polymorphism of plasminogen activator inhibitor-1 gene is associated with mortality in intensive care unit patients

with severe pneumonia. Anesthesiology 2009; 110: 1086-1091.

[31] Song Y, Lynch SV, Flanagan J, Zhuo H, Tom W, Dotson RH, Baek MS, Rubio-Mills A, Singh G, Kipnis E, Glidden D, Brown R, Garcia O and Wiener-Kronish JP. Increased plasminogen activator inhibitor-1 concentrations in bronchoalveolar lavage fluids are associated with increased mortality in a cohort of patients with pseudomonas aeruginosa. Anesthesiology 2007; 106: 252-261.

[32] Ware LB, Matthay MA, Parsons PE, Thompson BT, Januzzi JL and Eisner MD. Pathogenetic and prognostic significance of altered coagulation and fibrinolysis in acute lung injury/acute respiratory distress syndrome. Crit Care Med 2007; 35: 1821-1828.